



Spectroscopic Studies on TiO₂ Nanoparticles-Bovine Serum Albumin Interaction Under Visible Light and Dark Conditions

A. RAJESHWARI, KUMARI AMRITA, N. CHANDRASEKARAN and AMITAVA MUKHERJEE*

Centre for Nanobiotechnology, VIT University, Vellore-632 014, India

*Corresponding author: Tel: +91 416 2202620; E-mail: amit.mookerjee@gmail.com

Received: 2 May 2014;

Accepted: 15 July 2014;

Published online: 20 February 2015;

AJC-16894

Titania (TiO₂) nanoparticles are increasingly used in the consumer and industrial applications, but there is only a handful of studies regarding their interactions with protein molecules. The aim of the present study was to explore the interaction between TiO₂ nanoparticles and bovine serum albumin (BSA) under visible light and dark conditions. The UV-visible spectral studies showed a concentration dependent increase in absorption intensity under both the conditions denoting the formation of BSA-TiO₂ complex. The fluorescence quenching was noted upon addition of nanoparticles. The number of TiO₂ binding sites on bovine serum albumin were determined (light: 0.6, dark: 1.9) by Stern-Volmer plot. The circular dichroism analysis showed significant changes in α -helix content of the protein structure upon adding TiO₂. A significant reduction in reactive oxygen species generation by the TiO₂ nanoparticles was observed upon interaction with bovine serum albumin for both the conditions denoting the protein modulated decrease in photo reactivity of TiO₂ nanoparticles. This is one of the foremost studies to present a comparative estimation of the spectral changes upon interaction of bovine serum albumin with TiO₂ nanoparticles under visible light and dark conditions. In a direct implication to potential cytotoxicity of TiO₂ nanoparticles, this study confirms that interactions with bovine serum albumin can substantially reduce reactive oxygen species generation by the nanoparticles.

Keywords: TiO₂, Bovine serum albumin, Interaction, Visible light, Dark.

INTRODUCTION

Titania (TiO₂) nanoparticles have been widely used for a number of consumer and industrial applications in filters, cosmetics and electronics¹. The worldwide production of these nanoparticles is increasing by the day keeping in pace with its ever increasing demand. The size of the nanoparticles being comparable to most of the biomolecules is of potential importance for *in vivo* and *in vitro* biomedical research².

Serum albumins are the most abundant proteins in plasma and have major physiological functions^{3,4}. Among the serum albumins, bovine serum albumin is the most widely studied albumin due to its structural homology with human serum albumin (HSA) and its stability properties^{5,6}. Also, bovine serum albumin plays a major role in the transport and delivery of fatty acids, porphyrins and steroids.

Proteins such as bovine serum albumin or human serum albumin are generally added to dispersion media in order to increase stabilization of the media by preventing agglomeration of the nanoparticles⁷. In some cases, interaction of nanoscale objects with proteins leads to hazardous consequences, such as abnormal conformational changes leading to exposure of cryptic peptide epitopes or the appearance of abnormal functions caused by structural modifications^{8,9}. Therefore, the ability

to characterize the interaction of nanoparticles with proteins is of primary importance¹⁰.

Kathiravan *et al.*¹¹ have studied the interaction of ZnO nanoparticles with bovine serum albumin and observed that conformational changes occurred in bovine serum albumin due to its interaction with the metal oxide nanoparticle. Similarly, the investigation on the interaction of bovine serum albumin by ZnO nanoparticles^{12,13} and Al₂O₃ nanoparticles¹⁴ indicated existence of the static quenching and ground state complex formation. Song *et al.*¹⁵ have explored the adsorption behaviour of bovine serum albumin onto TiO₂, SiO₂ and Al₂O₃ nanoparticles without the disturbance of other ions. The bio-molecular interaction of colloidal TiO₂ with bovine serum albumin and human serum albumin under visible light has also been studied in terms of its fluorescence quenching^{16,17}.

The reactivity of TiO₂ nanoparticles has been widely reported being due to its photocatalytic nature¹⁸. Traditionally, TiO₂ nanoparticles have been regarded as chemically inert, nontoxic and biocompatible materials. However, recent studies have indicated that TiO₂ nanoparticles may impair the biological systems even in the absence of photoactivation^{19,20}. However, the investigations on TiO₂ nanoparticles interaction with bio-macromolecules in the presence and absence of photoactivation are still rare²¹.

To the best of our knowledge, there are no prior reports on the differential interactions of TiO₂ nanoparticles with bovine serum albumin in the presence and absence of light irradiation. Though it is quite well proven that the intracellular reactive oxygen species generation by the TiO₂ nanoparticles and consequent oxidative damage is one of the principal mechanisms of cytotoxicity of these nanoparticles, we could not find any previous report on the effects of BSA-TiO₂ nanoparticles interactions on the reactive oxygen species generation.

Therefore in the current study the differences (if any) in interaction of TiO₂ nanoparticles with bovine serum albumin under two conditions, namely (a) after illumination with visible light and (b) dark conditions were explored by means of various analytical techniques. The role of TiO₂ in modulating the conformation of bovine serum albumin was also investigated. On the other hand, the effect of bovine serum albumin onto the photo catalytic activity of the nanoparticles was studied through the reactive oxygen species assays under light irradiation and dark conditions.

EXPERIMENTAL

Dry titanium(IV) oxide nano powder was procured from Sigma Aldrich, USA. The physico-chemical parameters as reported by the supplier were: 99.7 % anatase with particle size < 25 nm. Dispersions of TiO₂ nanoparticles of different concentrations were freshly prepared by ultrasonic vibrations (130 W, 20 kHz) for 10 min for the interaction studies.

Bovine serum albumin (purity > 95 %), CAS No. 9048-46-8 was procured from Hi-Media, Pvt. Ltd., India and a concentration of 0.1 % was prepared with Millipore water. 2',7'-dichlorofluorescein-diacetate (DCFH-DA) was purchased from Sigma Aldrich, USA.

Characterization of as received nanoparticles: The morphology of the nanoparticles was observed using a transmission electron microscope (TEM, Philips CM 12, Netherlands). The size distribution of the nanoparticles was determined using a particle size analyzer (Brookhaven Instruments Corporation, USA).

Adsorption studies: The different concentrations of TiO₂ nanoparticles (12, 24, 36, 48 and 60 mg/L) were interacted with bovine serum albumin at a fixed concentration (0.1 %) for 0.5 h in test tubes placed in a rotary shaker at 300 rpm under visible light (incandescent light of intensity 120 W/m² and the distance between sample and light source was around 180 cm) and dark (absence of light and test tubes covered by aluminium foil) conditions. The interacted samples were then analyzed by the following techniques.

Particle size analysis: The hydrodynamic size of bovine serum albumin in the absence and presence of titania nanoparticles were recorded using a 90 plus particle size analyzer (Brookhaven Instruments Corporation, USA).

UV-visible spectroscopy: The UV-visible spectra of TiO₂ nanoparticles (different concentrations) and bovine serum albumin mixtures (3 mL) were recorded in a UV-visible spectrophotometer (Shimadzu UV-1700, Japan) in the range from 250 to 350 nm. The peak wavelength of the uninteracted TiO₂ nanoparticle was observed to be 330 nm. The absorbance was recorded using cell with 1 cm path length.

Fluorescence spectroscopy: Steady state fluorescence of the interacted samples (3 mL) under both light and dark conditions was measured using a spectrofluorometer (SL174 ELICO). The excitation wavelength was 290 nm and emission spectra were recorded in the range 300-550 nm. The fluorescence intensity was recorded using cell with 1 cm path length.

Fourier transform infra-red and circular dichroism spectroscopy: The TiO₂ nanoparticles at concentrations 12 and 60 mg/L of dispersed in Millipore water were interacted with 0.1 % of bovine serum albumin and incubated for 0.5 h in a rotary shaker at 300 rpm in light and dark conditions respectively. After incubation 15 mL of sample solutions were lyophilized for FTIR analysis. The various types of secondary protein structures were studied through FT-IR spectrometer (IR Affinity-1, Shimadzu, Japan) in diffuse reflectance mode.

For the circular dichroism analysis, 12 and 60 mg/L of TiO₂ dispersed in Milli-Q water was added to 0.1 % bovine serum albumin and the interaction was carried out in both light and dark condition. After 0.5 h of interaction, the samples were analyzed by circular dichroism (CD) spectroscopy (J-715, Jasco, Japan) using cell with 1 cm path length. The percentage of protein conformation change before and after interaction with TiO₂ was calculated using an in build software spectra manager 2.

Oxidative stress assessment

Determination of reactive oxygen species: The reactive oxygen species study was performed for the three concentrations of TiO₂ nanoparticles (12, 36, 60 mg/L). The test samples were prepared by interaction of 0.1 % of bovine serum albumin with TiO₂ nanoparticles dispersed in Millipore water and incubated for about 0.5 h under light and dark conditions. The samples were then centrifuged at 7000 rpm for 15 min, the supernatant was discarded and the pellet was collected and the final volume was made up to 5 mL. The control samples were made for each concentration. 5 µL of fluorescent dye 2',7'-dichlorofluorescein-diacetate (DCFH-DA) was added to control and test samples and after 0.5 h incubation the fluorescence was measured by spectrofluorometer (SL174, ELICO) with excitation and emission wavelengths of 485 and 530 nm, respectively²⁰.

RESULTS AND DISCUSSION

Characterization of as received TiO₂ nanoparticles: The transmission electron micrograph of TiO₂ nanoparticles suggested the presence of nearly spherical shape and the particle of size was in the range of 10-50 nm (Fig. 1). To validate the microscopic findings, the particle size distribution in aqueous solution was also determined by dynamic light scattering and the mean hydrodynamic diameter of the received nanoparticles was found to be around 50 nm and its poly dispersion index (PdI) was 0.13.

Interaction of TiO₂ nanoparticles with bovine serum albumin

Changes in hydrodynamic size upon formation of BSA-TiO₂ interaction: The hydrodynamic diameter of bovine serum albumin was reported to be 85 ± 1.6 nm. The hydrodynamic diameter of titanium dioxide at 12 mg/L concentration was 169 ± 4.9 nm and after the interaction, the mean diameter

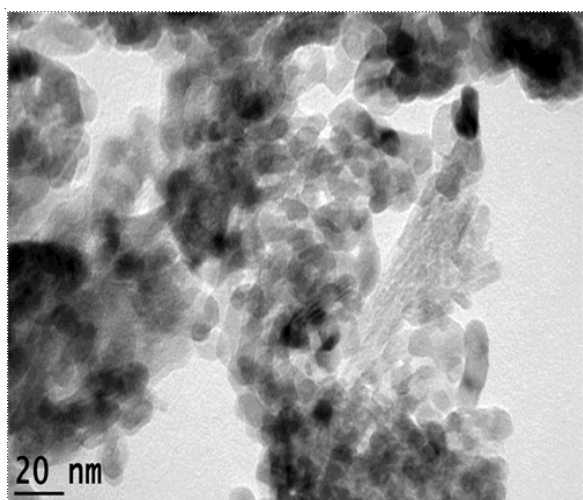


Fig. 1. Transmission electron micrograph of as-received TiO₂ nanoparticles

of the conjugate increased to about 431 ± 6.3 nm (light condition) and 454.7 ± 1.3 nm (dark condition). Similarly at 60 mg/L concentration the hydrodynamic diameter was 209 ± 7.5 nm and after the interactions with bovine serum albumin the conjugate diameter increased to 574 ± 2.4 nm under light condition and 615.3 ± 2.9 nm under dark condition. Table-1 clearly demonstrated the increase in mean hydrodynamic diameter of the BSA-TiO₂ conjugate as a function of increasing TiO₂ concentration. The aggregation in the presence of bovine serum albumin clearly was more enhanced compared to that of TiO₂ nanoparticles alone. The biomolecules have a significant contribution in modulating the stability of the nano dispersions²². For example, a stabilizing effect on carbon nanotube (CNT) dispersion was observed using 0.5 mg/mL of bovine serum albumin²³. However, the hydrodynamic size of the particles is dependent on multiple factors such as pH, concentration of bovine serum albumin and NaCl content in the solution²². In the present study, the destabilizing effect of bovine serum albumin on TiO₂ nanoparticles results in rapid aggregation and gravitational settling of the particles resulting in their reduced availability. Therefore decreased bio-reactivity and toxic impact of TiO₂ nanoparticles may be observed in the presence of bovine serum albumin under specific conditions.

TABLE-1
MEAN HYDRODYNAMIC SIZE OF TiO₂ NANOPARTICLES BEFORE AND AFTER INTERACTION WITH BOVINE SERUM ALBUMIN (0.1 %)

Conc. of TiO ₂ (mg/L)	Light condition		Dark condition	
	Before interaction	After interaction	Before interaction	After interaction
12	169±4.9 nm	431±6.3 nm	169±4.9 nm	454.7±1.3 nm
60	209 ±7.5 nm	574 ±24 nm	209 ±7.5 nm	615.3±2.9 nm

Absorption characteristics of BSA-TiO₂ system: The preliminary characterization of the BSA-nanoparticle interaction was performed using UV-visible spectroscopy. Bovine serum albumin showed a characteristic UV peak around 280 nm caused by the $\pi \rightarrow \pi^*$ transition of aromatic amino acid residues, tyrosine and tryptophan²⁴. Fig. 2a, b demonstrate the absorption spectrum of bovine serum albumin in the presence of TiO₂ nanoparticles (12-60 mg/L) when interacted under light and

dark conditions, respectively. A significant enhancement in the optical density was observed in the entire wavelength range scanned [200-500 nm] on the addition of nanoparticles in a concentration dependent manner with no notable change in the bovine serum albumin peak position. The observed increase was due to light scattering by the increased concentration and size of the nanoparticles²⁵. The concentration dependent increase in the scattering was due to consequent increase in the particle size upon interaction to bovine serum albumin, as substantiated by the DLS analysis (Table-1). No noticeable peak was observed in the aqueous dispersions containing TiO₂ nanoparticles (12-60 mg/L) in absence of bovine serum albumin (data not shown). It was also significant to note that the optical density of the BSA-TiO₂ system did not differ considerably under visible light from that under the dark conditions (Fig. 2a, b).

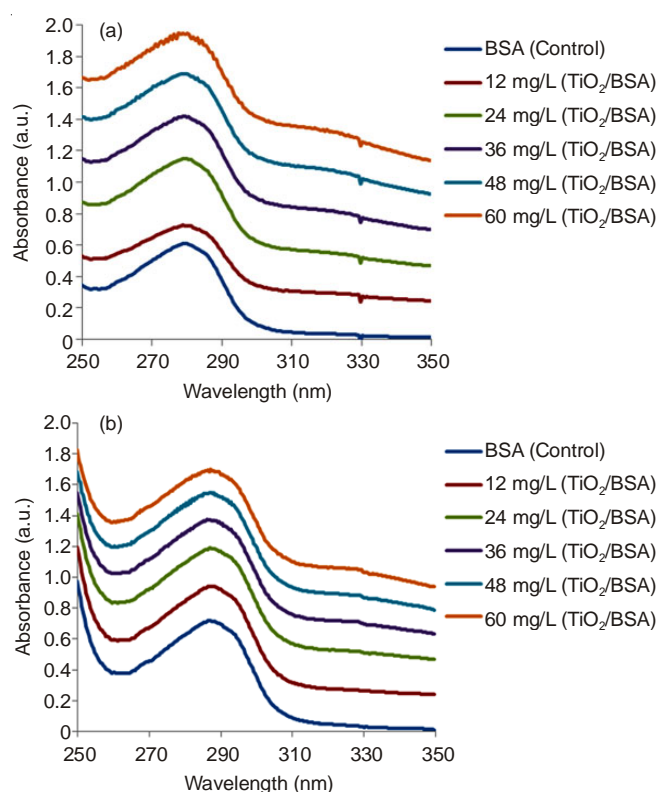


Fig. 2. UV-visible absorption spectrum of 0.1 % bovine serum albumin in the presence of various concentration TiO₂ nanoparticles (12, 24, 36, 48, 60 mg/L) under: (a) visible light condition; (b) dark condition

Fluorescence quenching on the addition of TiO₂ nanoparticles: Due to the strong light absorbance and nanoscale size of the particles, the light scattering effect and inner filter effect may cause deviation to fluorescence of TiO₂ nanoparticles-BSA system. Therefore, the fluorescence intensity was corrected for the absorption of excitation and reabsorption of emitted light by the following correction²⁶:

$$F_{\text{cor}} = F_{\text{obs}} \times e^{(A_{\text{ex}} + A_{\text{em}})/2} \quad (1)$$

where, F_{cor} and F_{obs} are the corrected and observed fluorescence intensities. A_{ex} and A_{em} are the absorbance of the system at excitation and emission wavelengths. The fluorescence quenching refers to any process that decreases the fluorescence intensity of a sample. Molecular interactions such as excited state reactions, molecular rearrangements, ground state

complex formation, energy transfer and collisional quenching can result in fluorescence quenching⁸. The fluorescence exhibited by bovine serum albumin has been studied to originate from tryptophan, tyrosine and phenyl alanine residues although intrinsic fluorescence is mainly contributed by tryptophan residues alone²⁷. Fig. 3a, b show the fluorescence spectra of BSA-TiO₂ nanoparticle complex under the visible light and dark conditions, respectively. The maximum emission was observed at 340 nm while the excitation was provided at 290 nm. The maximum emission wavelength shifted from 340 to 348 nm, suggesting that the molecular environment around the chromophore of bovine serum albumin may have been altered after the addition of nanoparticles (possibly denoting the changes in the conformation of the protein upon interaction)²⁸. The increase in the concentration of TiO₂ led to a corresponding decrease in the intensity of emission under both light and dark conditions, confirming intrinsic fluorescence quenching behavior of the particles. Kathiravan and Renganathan reported similar results under visible light conditions upon interaction of TiO₂ nanoparticles with bovine serum albumin¹⁶. They observed that the excited energy state of bovine serum albumin was greater than the band gap energy of TiO₂ and that the fluorescence of bovine serum albumin could be overlapped with the absorption of TiO₂ thereby paving the way for energy transfer from the excited state of bovine serum albumin to TiO₂.

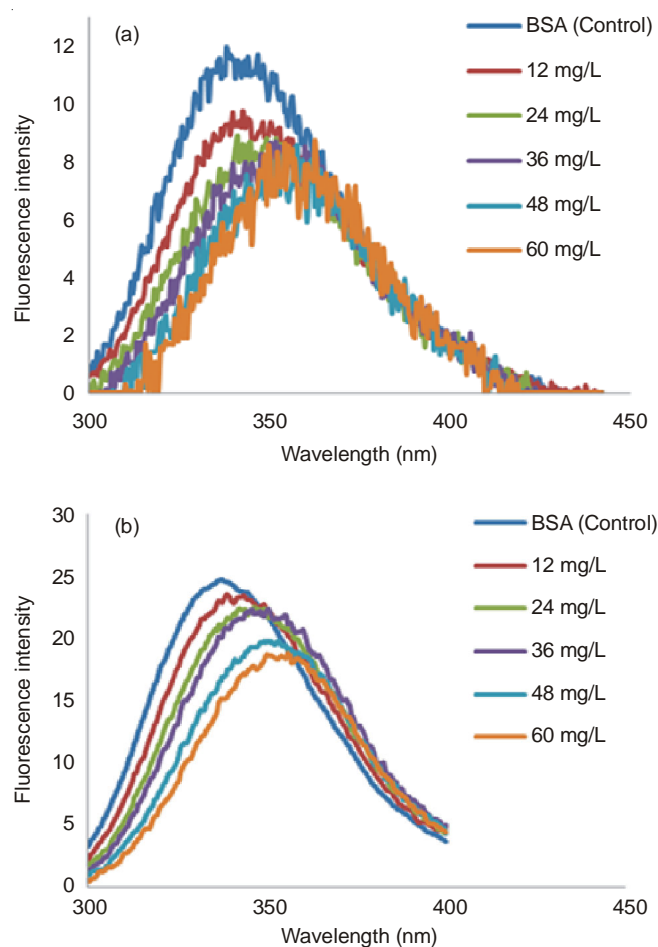


Fig. 3. Fluorescence spectra of 0.1 % bovine serum albumin in the presence of various concentration TiO₂ nanoparticles (12, 24, 36, 48, 60 mg/L) under: (a) visible light condition; (b) dark condition

Stern-volmer relation graph was also plotted using the following equation:

$$\frac{F_0}{F} = 1 + K_{sv}[Q] = 1 + Kq\tau[Q] \quad (2)$$

where, F_0 and F are the fluorescence intensities in the absence and the presence of a quencher at 340 nm, respectively, K_{sv} is the Stern-Volmer rate constant and related to Kq (bimolecular quenching rate constant) as shown in eqn. 2, τ is the average life time of bovine serum albumin which is 10^{-8} s¹⁶ and $[Q]$ the concentration of TiO₂ nanoparticle quencher. According to the Stern-Volmer description of binding, a plot of F_0/F as a function of $[Q]$ should be linear. The plot F_0/F vs. TiO₂ nanoparticles under visible light and dark conditions is shown in Fig. 4a and 4b demonstrating a fairly linear relationship in both the cases, which confirmed the presence of a single class of fluorophores equally accessible to the quencher⁸. The quenching rate constant was obtained from the slope (0.7×10^{12} L mol⁻¹ s⁻¹ and 0.47×10^{12} L mol⁻¹ s⁻¹ for the samples interacted under visible light and dark, respectively), assuming τ value of bovine serum albumin as 10^{-8} s.

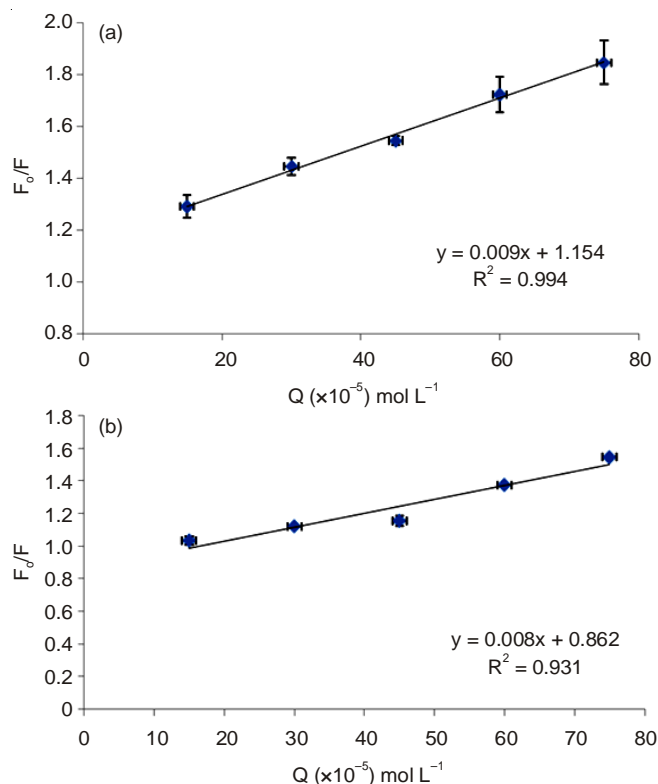


Fig. 4. A plot of F_0/F vs. TiO₂ nanoparticles for under: (a) light condition; (b) dark condition

The binding constant and the number of binding sites can be deduced from the following relationship:

$$\log \frac{F_0 - F}{F} = \log K_\alpha + n \log [Q] \quad (3)$$

where, K_α is the binding constant of TiO₂ with bovine serum albumin and n is the number of binding sites of TiO₂ with bovine serum albumin. Thus, the experimental values of $\log [(F_0 - F)/F]$ were plotted as a function of $\log [Q]$. Fig. 5a, b show the plot of $\log (F_0 - F)/F$ against $\log [Q]$ for the BSA-TiO₂

complex under visible light and dark conditions, respectively from which the values of K_{α} and n were deduced. The binding constant K_{α} was determined to be 1.98 and $5.90 \times 10^5 \text{ M}^{-1}$ while binding sites n was calculated to be 0.66 and 1.97 under visible light and dark conditions, respectively¹⁶. It can be noted that the binding constant K_{α} was quite lower compared with that observed for other BSA-ligands systems²⁹, which proved that the binding between TiO_2 and bovine serum albumin was not strong.

Though BSA- TiO_2 nanoparticle complex formation was confirmed from the fluorescence studies, no significant differences in quenching could be observed between the visible light and the dark conditions. This was further substantiated by the Stern-Volmer plot which indicated that the differences in the number of binding sites and binding constant of TiO_2 with bovine serum albumin under visible light than under dark conditions was not significant under the employed experimental conditions. This substantiates our prior observation from the absorption studies. In a clear deviation from the prior reports on BSA- TiO_2 nanoparticles interactions, the current study explored the possible differences in absorption and fluorescence characteristics of BSA- TiO_2 nanoparticle system under visible light and dark conditions.

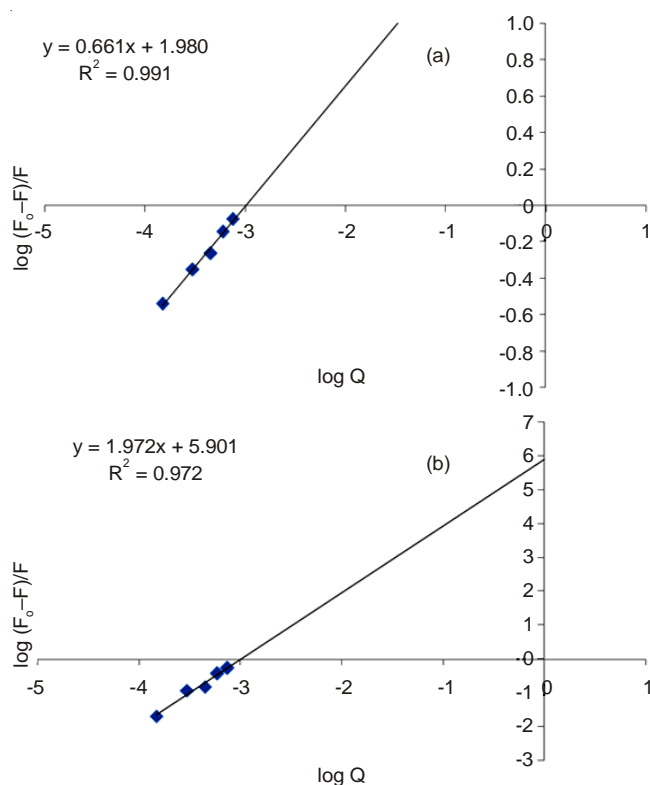


Fig. 5. A plot of $\log F_0-F/F$ vs. $\log [Q]$ under: (a) light condition; (b) dark condition

Changes in secondary structure of protein upon interaction with TiO_2 : The protein secondary structures were studied with the help of FT-IR and circular dichroism spectra. The Fig. 6a-e represents the FT-IR spectra of bovine serum albumin alone, BSA- TiO_2 conjugate in light and dark conditions for 12, 60 mg/L TiO_2 nanoparticles, respectively. The spectra for control bovine serum albumin shows the presence of amide I

and amide II peak positions in the region of 1700-1600 and 1548 cm^{-1} , respectively²⁸. It is significant to observe that amide I bands are more sensitive to changes in protein conformation¹¹. The presence of amide I band in the spectral region of 1620 cm^{-1} was observed, it is indicative of the exposed α -helical structure of the protein³⁰. No significant difference in the intensity of the amide I spectral region could be observed for BSA- TiO_2 complex (12, 60 mg/L) between both light and dark conditions.

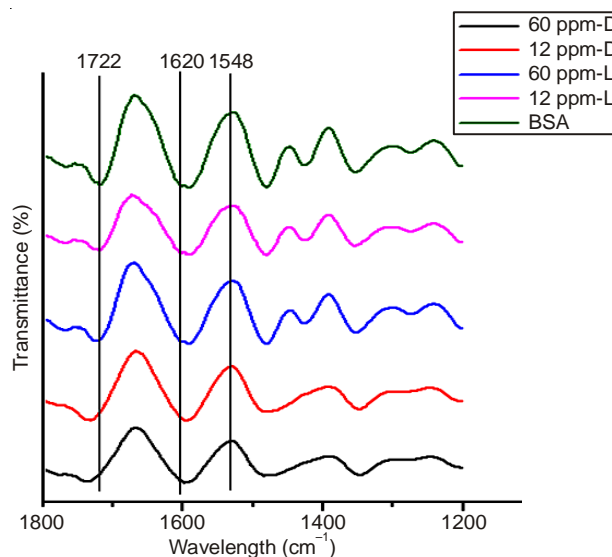


Fig. 6. FT-IR spectra of FT-IR spectra of 0.1 % bovine serum albumin and BSA- TiO_2 complex (12 and 60 mg/L) in the presence and absence of light

Fig. 7 represents the circular dichroism spectra of bovine serum albumin and BSA- TiO_2 complex (12 and 60 mg/L) under both visible light and dark conditions. Two strong negative bands in the UV region at 208 and 222 nm were observed in case of pure bovine serum albumin due to negative cotton effect and characteristic of a helical structure of protein³¹. The helix content of bovine serum albumin upon interaction with TiO_2 (60 mg/L, under visible light) increased from 38.7 to 60.7 while for that interacted under dark conditions, it increased from 47 to 64.1. The spectra of bovine serum albumin thus became more negative upon interaction with TiO_2 under both visible light and dark condition. The decrease in the α -helical content was possibly owing to the TiO_2 nanoparticles binding with amino acid residues of the polypeptide chain of protein. The results revealed the conformational change in bovine serum albumin due to its physiological environmental change after interaction with TiO_2 nanoparticles. But no significant changes were observed in the secondary structure between the two experimental conditions (light and non-illumination). This is an important observation given that no prior studies compared the possible conformational changes in bovine serum albumin upon interaction with TiO_2 nanoparticles under the visible light and the dark conditions.

Oxidative stress assessment: The oxidative stress induced by TiO_2 nanoparticles was assessed *via* production of reactive oxygen species, as a measure of the photo reactivity of the particles in aqueous suspension. The UV excited TiO_2 has for long been studied to generate reactive oxygen species and is

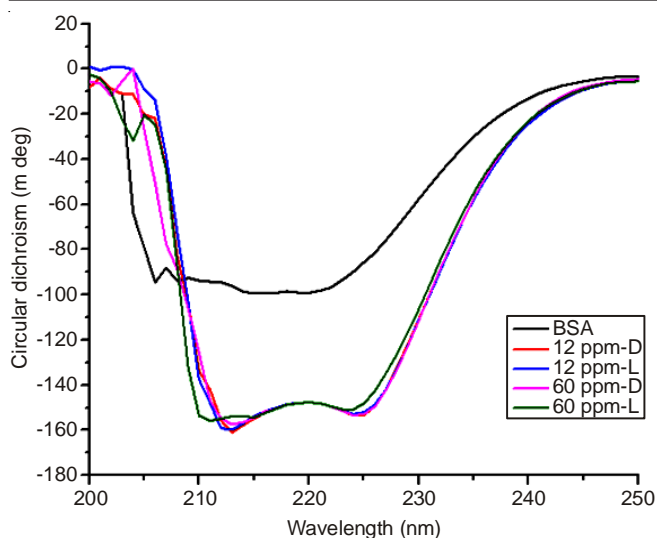


Fig. 7. Circular dichroism spectra of 0.1 % bovine serum albumin and BSA-TiO₂ complex (12 and 60 mg/L) in the presence and absence of light

observed to be a major contributor of cell damage, *i.e.*, cytotoxicity. Table-2 represents the reactive oxygen species assay under visible light and dark conditions, respectively. The reactive oxygen species levels were 90 ± 6.1 % under visible light and 79.3 ± 1.72 % under the dark conditions in the presence of 60 mg/L of TiO₂ alone. Though the primary reactive oxygen species level (in the absence of BSA) was considerably higher under visible light, a noticeable amount of reactive oxygen species was generated even under dark conditions. The results were consistent with previous reports of Burello and Worth who suggested that TiO₂ is capable of reactive oxygen species generation irrespective of UV excitation as the position of its conduction bands lies in the range of biological redox potentials¹⁹. The increased primary reactive oxygen species generation under light conditions (as compared to dark) can be attributed to the photo reactivity of TiO₂ nanoparticles²⁰.

Conc. of TiO ₂ (mg/L)	Light condition		Dark condition	
	Control (TiO ₂) (%)	BSA-TiO ₂ complex (%)	Control (TiO ₂) (%)	BSA-TiO ₂ complex (%)
12	27.3 0±0.46	4.50±0.88	21.19±0.13	3.51±2.02
36	60.30±3.16	6.59 ±1.83	59.53±0.1	4.56±3.66
60	79.33±2.43	11.46±3.52	99.03±0.2	7.03±0.89

The formation of TiO₂-BSA complex led to a considerable decrease in reactive oxygen species level under both visible light and dark conditions when compared to the control. The results were in accordance with previous studies by our group on reactive oxygen species release upon interaction of TiO₂ with bacterial cells under the visible light and dark conditions²⁰. Furthermore, the level of reactive oxygen species was found to be lesser for the complex which was interacted under visible light than under the dark conditions. The reactive oxygen species level was 7.82 ± 0.85 % under visible light while it was 11.46 ± 0.25 % under dark conditions in the presence of

60 mg/L TiO₂ and 0.1 % bovine serum albumin. This is one of the first reports with regard to the possible effects of bovine serum albumin on reactive oxygen species generation by the TiO₂ nanoparticles, which has direct correlation with the cytotoxicity potential of these nanoparticles.

Conclusion

In absence of any prior report the present study explores the differential interactions of TiO₂ nanoparticles with bovine serum albumin in the presence and absence of light irradiation by different spectroscopic methods including UV-visible spectroscopy, fluorescence spectroscopy, FT-IR and circular dichroism. The results indicate the concentration dependent increase in scattering by the nanoparticles upon interaction with bovine serum albumin and quenching of intrinsic protein fluorescence through energy transfer. The analyses of FT-IR and circular dichroism spectra confirmed that the secondary structure of bovine serum albumin was affected by the presence of TiO₂ nanoparticles, though no significant change was observed between the light and non-illumination conditions. The present study is also among the first ones to report that the formation of BSA-TiO₂ complex led to a significant decrease in the reactive oxygen species generation under both the conditions indicating that the protein binding possibly reduced the photo-reactivity of TiO₂ nanoparticle. The current findings can further be extrapolated to study the mechanistic aspects of the interactions of different photo-catalytic nanoparticles with various biomacromolecules of interest.

ACKNOWLEDGEMENTS

The authors acknowledge to Dr. G. Jayaraman, VIT University for extending the Circular Dichroism facility.

REFERENCES

- S. Kaewgun, C.A. Nolph, B.I. Lee and L.Q. Wang, *Mater. Chem. Phys.*, **114**, 439 (2009).
- A. Ravindran, A. Singh, A.M. Raichur, N. Chandrasekaran and A. Mukherjee, *Colloids Surf. B*, **76**, 32 (2010).
- D.D. Carter and J.X. Ho, *Adv. Protein Chem.*, **45**, 153 (1994).
- R.E. Olson and D.D. Christ, *Annu. Rep. Med. Chem.*, **31**, 327 (1996).
- F. Rasoulzadeh, D. Asgari, A. Naseri and M.R. Rashidi, *DARU*, **18**, 179 (2010).
- C. Wang, Q.-H. Wu, Z. Wang and J. Zhao, *Anal. Sci.*, **22**, 435 (2006).
- R. Tantra, J. Tompkins and P. Quincey, *Colloids Surf. B*, **75**, 275 (2010).
- J. Mariam, P.M. Dongre and D.C. Kothari, *J. Fluoresc.*, **21**, 2193 (2011).
- A.A. Shemetov, I. Nabiev and A. Sukhanova, *ACS Nano*, **6**, 4585 (2012).
- P. Bihari, M. Vippola, S. Schultes, M. Praetner, A.G. Khandoga, C.A. Reichel, C. Coester, T. Tuomi, M. Rehberg and F. Krombach, *Part. Fibre Toxicol.*, **5**, 14 (2008).
- A. Kathiravan, G. Paramaguru and R. Renganathan, *J. Mol. Struct.*, **934**, 129 (2009).
- M. Bardhan, G. Mandal and T. Ganguly, *J. Appl. Phys.*, **106**, 034701 (2009).
- A. Bhogale, N. Patel, P. Sarpotdar, J. Mariam, P.M. Dongre, A. Miotello and D.C. Kothari, *Colloids Surf. B*, **102**, 257 (2013).
- A. Rajeshwari, S. Pakrashi, S. Dalai, V. Madhumita, V. Iswarya, N. Chandrasekaran and A. Mukherjee, *J. Lumin.*, **145**, 859 (2014).
- L. Song, K. Yang, W. Jiang, P. Du and B. Xing, *Colloids Surf. B*, **94**, 341 (2012).
- A. Kathiravan and R. Renganathan, *Colloids Surf. A*, **324**, 176 (2008).
- A. Kathiravan, S. Anandan and R. Renganathan, *Colloids Surf. A*, **333**, 91 (2009).
- T.J. Battin, F.V.D. Kammer, A. Weilharter, O. Ottofuelling and T. Hofmann, *Environ. Sci. Technol.*, **43**, 8098 (2009).

19. E. Burello and A.P. Worth, *Nanotoxicology*, **5**, 228 (2011).
20. S. Dalai, S. Pakrashi, R.S.S. Kumar, N. Chandrasekaran and A. Mukherjee, *Toxicol. Res.*, **1**, 116 (2012).
21. W. Sun, Y. Du, J. Chen, J. Kou and B. Yu, *J. Lumin.*, **129**, 778 (2009).
22. D. Elgrabli, S. Abella-Gallart, O. Aguerre-Chariol, F. Robidel, F. Rogerieux, J. Boczkowski and G. Lacroix, *Nanotoxicology*, **1**, 266 (2007).
23. J.Y. Jun, H.H. Nguyen, S.-Y.-R. Paik, H.S. Chun, B.-C. Kang and S. Ko, *Food Chem.*, **127**, 1892 (2011).
24. J. Huang, Y.Z. Yuan and H. Liang, *Sci. China Series B*, **46**, 387 (2003).
25. S.K. Ghosh and T. Pal, *Chem. Rev.*, **107**, 4797 (2007).
26. J.R. Lakowicz, *Principles of Fluorescence Spectroscopy*, Plenum Press, New York (1983).
27. D. Li, Y. Wang, J. Chen and B. Ji, *Spectrochim. Acta A*, **79**, 680 (2011).
28. G.Z. Chen, X.Z. Huang, J.G. Xu, Z.Z. Zheng and Z.B. Wang, *Methods of Fluorescence Analysis*, Science Press, Beijing, edn 2 (1990).
29. S. Dubeau, P. Bourassa, T.J. Thomas and H.A. Tajmir-Riahi, *Biomacromolecules*, **11**, 1507 (2010).
30. A. Papadopoulou, R.J. Green and R.A. Frazier, *J. Food Agric. Chem.*, **53**, 158 (2005).
31. N. Greenfield and G.D. Fasman, *Biochemistry*, **8**, 4108 (1969).